Analysis of Airfoil Leading-Edge Separation Bubbles

V. N. Vatsa* and J. E. Carter†
United Technologies Research Center, East Hartford, Connecticut

A local inviscid-viscous interaction technique has been developed for the analysis of low-speed, airfoil leading-edge transitional separation bubbles. In this analysis an inverse boundary-layer finite difference scheme is solved iteratively with a Cauchy integral representation of the inviscid flow which is assumed to be a linear perturbation to a known global viscous airfoil solution. Favorable comparisons with data indicate the overall validity of the present localized interaction approach. In addition, numerical tests were performed to test the sensitivity of the computed results to the limits on the Cauchy integral and the location of the transition region.

Nomenclature

c = airfoil chord
c_f = skin friction coefficient
f = perturbation stream function
F = velocity ratio, u/u_e
g = total enthalpy ratio, H/H_e
H = total enthalpy
L = reference length
M = Mach number
m = perturbation mass flow
N = coordinate measured normal to reference displacement surface from the body surface
Pr = Prandtl number
Pr_t = turbulent Prandtl number
Re = reference Reynolds number
s,n = coordinates along and normal to the reference displacement surface, respectively
u,v = velocity components parallel and normal to the reference displacement surface, respectively
V = transformed normal velocity in Prandtl transposition theorem
β = pressure gradient parameter
λ = streamwise intermittency function
δ^* = displacement thickness
ϵ = eddy viscosity coefficient
η = transformed normal coordinate
μ = molecular viscosity coefficient
ξ = transformed tangential coordinate
ρ = density
ψ = stream function

Subscripts

e = edge of boundary layer
I = inviscid
ref = reference solution
t_1 = start of transition
t_2 = end of transition
v = viscous
1 = start of interaction region
2 = end of interaction region
∞ = freestream

Superscripts

$( )'$ = perturbation quantity
i = global viscous-inviscid iteration counter

Presented as Paper 83-0300 at the AIAA 21st Aerospace Sciences Meeting, Reno, Nev., Jan. 10-13, 1983; submitted Feb. 1, 1983; revision received Feb. 6, 1984.

*Research Engineer; presently, NASA Langley Research Center, Hampton, Va. Member AIAA.
†Manager, Computational Fluid Dynamics. Member AIAA.

Introduction

IF the Reynolds number is sufficiently low so that the boundary layer remains laminar up to the minimum pressure point on an airfoil, separation generally occurs almost immediately downstream of this point since laminar boundary layers, in contrast with turbulent flows, are extremely sensitive to adverse pressure gradients. A separation bubble forms in which a recirculating streamline pattern is bounded by a shear layer which generally undergoes transition from laminar to turbulent flow. Further downstream the turbulent mixing between the shear layer and the lower dead air region results in entrainment of higher energy air which energizes the flow near the surface thereby resulting in flow reattachment with subsequent turbulent boundary-layer flow downstream. Tani,[1] in his excellent article on airfoil bubble separations, points out that airfoil transitional separation bubbles are generally classified as either long or short. Tani designates long bubbles as those which result in a pressure distribution which is radically different from that in inviscid flow whereas a short bubble, which occupies a few percent of the chord, has only a local effect on the pressure distribution. The focus of the present work is the development of a prediction technique for short separation bubbles near airfoil leading edges.

There have been numerous experimental investigations conducted, such as the work of Bursnall and Loftin,[2] Gault,[3] Gaster,[4] and more recently that of Mueller and Batill[5] to provide information on the flow in the neighborhood of laminar transition separation bubbles. Experimental data such as this has been used by Owen and Klanfer,[6] Horton,[7] and Roberts[8] to deduce semiempirical criteria for the growth and bursting of laminar separation bubbles. At the present time airfoil analysis codes, such as the NASA-Lockheed multielement airfoil code[9] and the GRUMFOIL code,[10] use simple criteria such as these to detect the occurrence of laminar separation bubbles and whether or not bursting occurs. In these analyses, if laminar separation is detected without bursting then the flow is assumed to undergo immediate transition to turbulent flow with a jump discontinuity in the boundary-layer parameters such as shape factor and skin friction.

With the recent theoretical developments in a boundary-layer and viscous-inviscid interaction theory for separated flow, there have been several analytical investigations[11-15] conducted to provide a detailed description of the flow process in a laminar transitional separation bubble. These studies have been based on both finite difference and integral techniques for the boundary-layer equations which are solved iteratively with a Cauchy integral representation of the perturbed inviscid flow. Most of this work has been focused on midchord separation bubbles, although some results were

shown by Crimi and Reeves[12] and Pletcher et al.[13] for leading-edge separation bubbles.

The overall objective of the present paper, which is a condensation of the work presented in Ref. 16, is the development of an analytical procedure for predicting airfoil leading-edge laminar separation bubbles. Prior to bursting, the streamwise extent of the separation bubble is only a few percent of chord; hence in a manner similar to the previous theoretical approaches discussed above, a local viscous-inviscid interaction analysis has been developed for the immediate vicinity of the separation bubble. However, in contrast with these previous efforts, the present perturbation approach is based on the use of a global airfoil viscous analysis which provides the reference pressure and displacement thickness as input for the local leading-edge interaction analysis. In this manner, the global flowfield around the airfoil, including the wake, is taken into account. In the present study, the viscous airfoil analysis (GRUMFOIL code) of Melnik et al.[10] has been used. This analysis solves for the viscous flow over a lifting airfoil by an iterative solution of the conservative form of the full potential equation combined through classical displacement thickness coupling with an integral representation of the boundary-layer equations. Special analytical treatment is included near the trailing edge to account for normal pressure gradients which can occur in the viscous layer in this region.

Computations are presented for several airfoils for which experimental data were available. In addition, comparison is made with the benchmark experimental data obtained by Gaster.[4] Overall, the computed solutions are in good agreement with available data; not surprisingly it was observed that the solutions were quite sensitive to the transition model employed in the present paper. Since the major thrust of the present work was to demonstrate the feasibility of a local interaction model used in conjunction with a global airfoil analysis, a simple streamwise intermittency function was found sufficient to represent the transition from laminar to turbulent flow for the cases studied here.

Viscous-Inviscid Interaction Analysis

The present analysis for airfoil leading-edge separation bubbles is based on a viscous-inviscid interaction technique in which the boundary-layer equations are solved iteratively with an inviscid analysis through displacement thickness coupling. As mentioned in the Introduction, the focus of the current effort is the analysis of closed laminar transitional separation bubbles which are known from the experimental studies cited previously to occupy only a few percent of the airfoil chord. Since the resultant interaction is highly localized, it was decided to treat the leading-edge transitional bubble problem as a linear perturbation to a known global airfoil solution. The use of a localized interaction analysis, despite the overall approximation inherent in a perturbation approach, permits an accurate analysis of the local flowfield structure, in contrast with the extremely difficult problem of trying to resolve this small-scale phenomenon while simultaneously solving the global airfoil flowfield. Previous approaches have treated the airfoil separation bubble as a perturbation to an approximate global inviscid solution for the airfoil. In contrast, the present approach includes viscous effects in the airfoil global solution. This is important since it is well known that at high angles of attack, where transitional bubbles occur, the turbulent interaction at the airfoil trailing edge and wake influence the entire airfoil pressure including the location of the stagnation point and the level of suction pressure, which are the flow conditions upstream of the leading-edge transitional bubble. In the present investigation the GRUMFOIL viscous airfoil analysis[10] was used to establish the reference pressure and displacement thickness distributions which were then input to the local interaction analysis described in this section. The local inviscid analysis is discussed first, followed by a description of the boundary-layer analysis and the iteration procedure used to couple these two analyses.

Inviscid Analysis

The displacement surface which results from the laminar separation bubble is shown schematically in Fig. 1 for the flow near the airfoil leading edge. It is assumed in the present analysis that the viscous displacement surface is represented by a distribution of sources placed along the reference displacement surface which is also shown in Fig. 1. The reference displacement surface is that predicted by the global airfoil analysis in which instantaneous transition is assumed to occur at the laminar separation point, thereby eliminating the formation of a laminar separation bubble. The viscous-inviscid iteration procedure keys on the inviscid velocity along the interaction displacement surface which, in the present analysis, is approximated as

$$u_e(s) = u(s,0) = u_{\text{ref}}(s,0) + u'(s,0) \tag{1}$$

where u_{ref} is the velocity component obtained from the global airfoil analysis for the flow over the reference displacement surface, and u' is the perturbation velocity induced by the local transitional bubble. The perturbation velocity is given by the Cauchy integral

$$u'(s,0) = \frac{1}{\pi}\int_{s_1}^{s_2} \frac{\mathrm{d}}{\mathrm{d}\xi}\left[u_e(\delta^* - \delta^*_{\text{ref}})\right]\mathrm{d}\xi \Big/ (s-\xi) \tag{2}$$

in which the source strength is proportional to the streamwise rate of growth of the difference between the total and reference displacement thicknesses. Equation (2) is only an approximate solution since it assumes that the sources are distributed along a straight line, whereas near the airfoil nose the reference displacement surface, which closely follows the airfoil shape, is highly curved. However, since the interaction length is very short, it is assumed that over the interaction region the reference displacement surface curvature is a higher order contribution which has been ignored in the present investigation.

The Cauchy integral given in Eq. (2) is evaluated from s_1 to s_2 which is the region of strong interaction that results from the presence of the local transitional separation bubble. The lower limit, s_1, on the Cauchy integral is placed sufficiently far upstream of the interaction region where the source strength is zero, since the interaction displacement surface merges smoothly with the reference displacement surface in this region as shown in Fig. 1. The placement of the down-

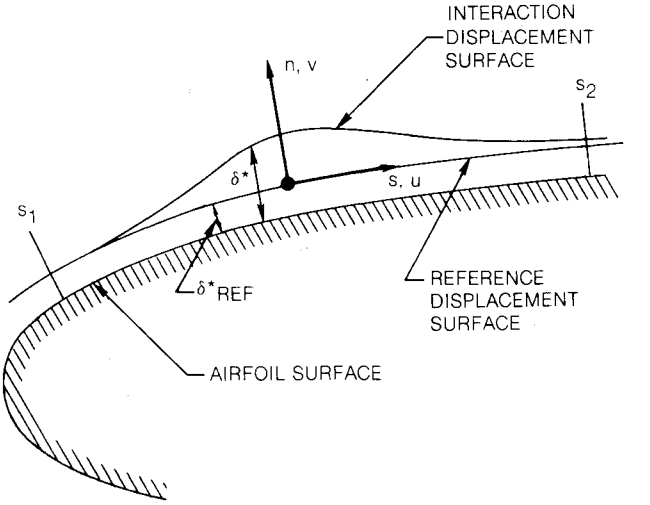

Fig. 1 Local interaction region coordinate system.

stream limit is somewhat more complicated since the interacted displacement surface does not merge into the reference displacement surface downstream of the interaction region. This result is expected since the presence of the transitional separation bubble results in a thicker downstream turbulent boundary layer than that obtained from the global airfoil analysis. In the latter analysis, the transitional separation bubble is eliminated by placing transition at the laminar separation point. However, it was found in the present calculations that the source strength is very close to zero downstream of the bubble since the interacted and reference displacement thicknesses are nearly parallel to each other. Numerical tests were performed which confirmed the insensitivity of the local interaction analysis to the values of the limits s_1 and s_2 provided they were placed sufficiently far enough upstream and downstream, respectively, of the interaction region. It is noted that the present perturbation procedure, which is based on the use of a reference displacement surface, considerably simplifies the choice of these limits over that used by other investigators[11-15] in which the Cauchy integral was used to predict the disturbance field due to the total interaction displacement surface. In the latter case the reference solution is the inviscid flow over the airfoil.

The Cauchy integral given in Eq. (2) is evaluated numerically using a second-order scheme developed by Napolitano et al.[17] In this procedure, the integration region, $s_1 \le s \le s_2$, is subdivided into $I_{\max}$ grid points with the complete integral written as the sum of integrals over these subintervals to yield the perturbation velocity at each grid point. This numerical procedure permits the use of a nonuniform mesh distribution which was used in the present problem to concentrate grid points near the center of the interaction region in order to adequately resolve the high gradient phenomena which occurs as the flow undergoes transition from laminar to turbulent flow. The same surface grid point distribution was used in both the inviscid and boundary-layer analyses thereby avoiding the interpolation between these two solutions in the interaction calculations.

Viscous Analysis

The viscous solution technique used in the present investigation is the inverse boundary-layer procedure presented by Carter[18] for the analysis of separated flows. Although the inviscid analysis discussed in the previous section has been limited to low-speed flow, the boundary-layer analysis used in the present study was adapted from earlier work which was for compressible flow. Thus, the fully compressible boundary-layer analysis is presented here.

It was shown by Werle and Verdon[19] that the nondimensional boundary-layer equations can be written in terms of the reference displacement surface coordinate system shown in Fig. 1 as follows:

$$\frac{\partial \rho u}{\partial s} + \frac{\partial \overline{\rho v}}{\partial n} = 0 \tag{3}$$

$$\rho u \frac{\partial u}{\partial s} + \overline{\rho v} \frac{\partial u}{\partial n} = \rho_e u_e \frac{du_e}{dx} + \frac{\partial}{\partial n}\left[\mu \frac{\partial u}{\partial n} - \rho \overline{u'v'}\right] \tag{4}$$

$$\rho u \frac{\partial H}{\partial s} + \overline{\rho v} \frac{\partial H}{\partial n} = \frac{\partial}{\partial n}\left[\frac{\mu}{Pr}\frac{\partial H}{\partial n} - \rho \overline{v'H'} + \mu\left(1 - \frac{1}{Pr}\right) u \frac{\partial u}{\partial n}\right] \tag{5}$$

The v component of velocity and the n coordinate are scaled in the usual manner by $\sqrt{Re_{\infty,c}}$, where $Re_{\infty,c}$ is the Reynolds number based on the freestream flow conditions and the airfoil chord. The boundary conditions imposed on these governing equations are:

$$n = -\delta^*_{\text{ref}} \quad u = v = 0, \quad H \text{ or } \frac{\partial H}{\partial n} \text{ specified} \tag{6}$$

$$n \to \infty \quad u \to u_e, \quad H \to H_e \tag{7}$$

The Reynolds stresses are related to the mean flow by

$$-\rho \overline{u'v'} = \epsilon \lambda \frac{\partial u}{\partial n}, \qquad -\rho \overline{v'H'} = \frac{\epsilon \lambda}{Pr_t}\frac{\partial H}{\partial n} \tag{8}$$

where ϵ is the eddy viscosity coefficient for which the Cebeci-Smith[20] two-layer model for fully turbulent flows was used. The transition from laminar to turbulent flow as modeled by the use of a streamwise intermittency function $\lambda(s)$ which varies from 0 to 1 over a specified region. The treatment of the transition region will be discussed in more detail in the next section.

Werle and Verdon[19] showed that it is convenient to transform the boundary-layer equations with the Prandtl transposition theorem which is given by

$$s = s, \qquad N = n + \delta^*_{\text{ref}}, \quad V = v + u\frac{d\delta^*_{\text{ref}}}{ds} \tag{9}$$

where N is a transformed normal coordinate measured from the airfoil surface perpendicular to the reference displacement surface. In Ref. 19, it is shown that the form of the boundary-layer equations is unchanged by this transformation and the same surface boundary conditions, Eq. (6), are imposed at $N = 0$.

The development of the inverse formulation begins by transforming the equations, expressed in primitive variables, by the following transformation of the independent variables:

$$\xi = \int_0^x \rho_e \mu_e u_e ds \qquad \eta = \frac{1}{\delta^*}\int_0^N \frac{\rho}{\rho_e} dN \tag{10}$$

which is quite similar to the Levy-Lees transformation. It is helpful to scale the normal coordinate by the displacement thickness in strongly interacting flows since this step insures that the boundary-layer thickness is approximately constant in the transformed coordinate. The prescribed displacement thickness distribution is inserted into the present boundary-layer formulation by the introduction of the stream function

$$\rho u = \frac{\partial \psi}{\partial N} \qquad \rho v = -\frac{\partial \psi}{\partial s} \tag{11}$$

which automatically satisfies the continuity equation. The value of the stream function at the boundary-layer edge is written in terms of the displacement thickness

$$\psi \to \rho_e u_e (N - \delta^*) \tag{12}$$

where

$$\delta^* = \int_0^\infty \left(1 - \frac{\rho u}{\rho_e u_e}\right) dN \tag{13}$$

Then with the definitions

$$m = \rho_e u_e \delta^* \quad h = \int_0^\infty \left(\frac{\rho_e}{\rho} - 1\right) d\eta \tag{14}$$

the edge value of the stream function can be written as

$$\psi \to m(\eta - 1 + h) \quad \text{as} \quad \eta \to \infty \tag{15}$$

A perturbation stream function is defined as

$$\tilde{f} = (1/\sqrt{2\xi})\,[\psi - Fm(\eta - 1 + h)] \text{ with } F = u/u_e \tag{16}$$

such that $\tilde{f} \to 0$ as $\eta \to \infty$ for a prescribed m. Note that in the transformed inverse formulation the perturbation mass flow m is prescribed and not just the displacement thickness.

Transformation of the compressible boundary-layer equations with Eq. (10) and the introduction of the perturbation stream function defined in Eq. (16) results in the following set of governing equations:

$$\frac{\partial \tilde{f}}{\partial \eta} = \frac{m}{\sqrt{2\xi}}(1-\eta-h)\frac{\partial F}{\partial \eta} \tag{17}$$

$$m^2 F\frac{\partial F}{\partial \xi} - m\frac{\partial}{\partial \xi}[\sqrt{2\xi}\tilde{f} + mF(\eta - 1 + h)]\frac{\partial F}{\partial \eta}$$

$$= m^2\beta(g - F^2) + \frac{\partial}{\partial \eta}\left[\left(1+\frac{\epsilon}{\mu}\right)\ell\frac{\partial F}{\partial \eta}\right] \tag{18}$$

$$m^2 F\frac{\partial g}{\partial \xi} - m\frac{\partial}{\partial \xi}[\sqrt{2\xi}\tilde{f} + mF(\eta - 1 + h)]\frac{\partial g}{\partial \eta}$$

$$= \frac{1}{Pr}\frac{\partial}{\partial \eta}\left[\ell\left(1+\frac{\epsilon}{\mu}\frac{Pr}{Pr_t}\right)\frac{\partial g}{\partial \eta}\right]$$

$$+ \frac{(\gamma-1)M_e^2}{1+\frac{\gamma-1}{2}M_e^2}\frac{\partial}{\partial \eta}\left[\ell\left(1-\frac{1}{Pr}\right)F\frac{\partial F}{\partial \eta}\right] \tag{19}$$

where

$$g = \frac{H}{H_e} \qquad \beta = \frac{1}{M_e}\frac{dM_e}{d\xi} \qquad \ell = \frac{\rho\mu}{\rho_e\mu_e} \tag{20}$$

Equations (17-20) are solved for F, g, $\tilde{f}$, and β for a prescribed streamwise distribution of m subject to the following boundary conditions:

$$\eta = 0 \quad F = \tilde{f} = 0 \quad g = g_w \quad \text{or} \left.\frac{\partial g}{\partial \eta}\right|_w \text{specified}$$

$$\eta \to \infty \quad F = g \to 1 \quad \text{and} \; \tilde{f} \to 0 \tag{21}$$

These equations can also be solved in the direct mode with β prescribed and the outer boundary condition $\tilde{f} = 0$ eliminated. In this case if m is set equal to $\sqrt{2\xi}$ then the usual Levy-Lees formulation is deduced with the only difference being that the normal component of velocity has been rewritten in terms of the stream function. In the inverse case the unknown pressure gradient parameter is deduced simultaneously with the remainder of the solution. The numerical solution of these equations for both the direct and inverse modes is based on an implicit finite difference technique which is first-order accurate in the stream direction and second-order accurate in the normal direction. The details of the numerical scheme are presented by Carter.[21] In regions of reversed flow, use has been made of the Reyhner Flügge-Lotz[22] approximation in which the streamwise convection terms are set to zero to eliminate the instability which occurs in solving the boundary-layer equations in a direction opposite to that of the flow.

Transition Model

The prediction of the transition process as a flow changes from laminar to turbulent remains one of the most challenging problems in fluid dynamics despite the enormous attention given to this problem over the past 60 years. The prediction of transition is particularly difficult in an airfoil leading-edge separation bubble since it occurs in a region where the viscous flow is strongly interacting with the local inviscid flow. To the authors' knowledge, there have been only a few limited efforts, such as the work of van Ingen,[23] which have attempted to analyze the instability process which leads to transition from laminar to turbulent flow in a separated shear layer bounding a closed recirculation region. Since the objective of the present investigation was the development and demonstration of a viscous-inviscid interaction method for the analysis of airfoil leading-edge transitional separation bubbles, a simple forced transition model in which the onset and length of transition were prespecified was used to obtain the results presented herein.

The forced transition model used in the present analysis is based on the streamwise intermittency distribution which was established by Dhawan and Narasimha[24] by correlating a number of experimental studies of flows undergoing transition. For the present study this intermittency function has been written as

$$\lambda = 1 - \exp\left[-4.65\left(\frac{s - s_{t_1}}{s_{t_2} - s_{t_1}}\right)^2\right] \tag{22}$$

where s_{t_1} is the streamwise position where transition begins and s_{t_2} is the end of transition which was assumed to occur at $\lambda = 0.99$. In the present calculations, the values of s_{t_1} and s_{t_2} were deduced from the experimental data and input to Eq. (22) to complete the specification of $\lambda(s)$. An example of the sensitivity of the computed results to the intermittency function is presented in the Results and Discussion Section.

Interaction Iteration Procedure

The present analysis is based on a viscous-inviscid iteration technique which was presented previously by Carter[25] and is outlined in Fig. 2. This procedure, which has been referred to as a semi-inverse technique by LeBalleur,[26] combines an inverse boundary-layer technique with a direct inviscid analysis via the update procedure shown in Fig. 2. The key feature of this iteration procedure is the simple update formula

$$m^{i+1} = m^i\left[1 + \omega\left(\frac{u_{e_V}}{u_{e_I}} - 1\right)\right] \tag{23}$$

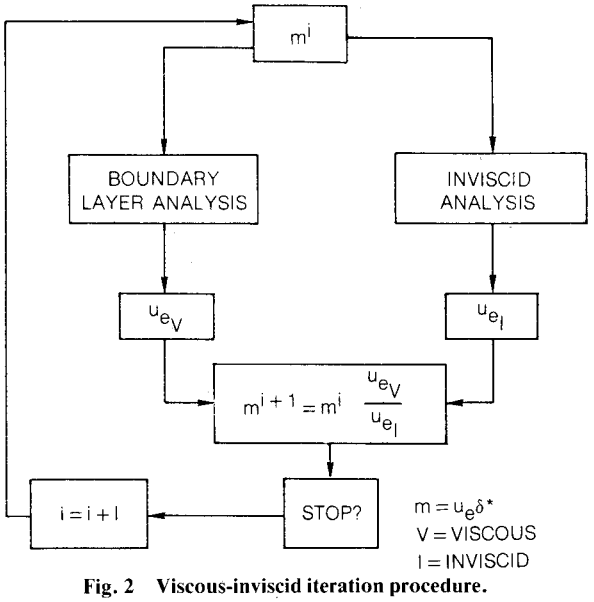

Fig. 2 Viscous-inviscid iteration procedure.

which permits an inverse boundary-layer analysis to be easily linked to an inviscid analysis which accounts for displacement thickness effects. For simplicity the update formula is shown in Fig. 2 with the relaxation factor ω set equal to one. This interaction iteration procedure, shown in Fig. 2, is general and has been used in a number of other studies[13,19,27-29] in which a variety of inverse boundary-layer and direct inviscid solution procedures have been employed. It was found by Pletcher et al.[13] that convergence could be accelerated by making several inner-loop passes through the Cauchy integral and the update formula with the boundary-layer prediction and the edge velocity u_{e_v} frozen at its current global iteration value. This technique was used in the present calculations with three inner-loop passes and was found to accelerate the global convergence rate by a factor of 3 with a 50% reduction in computer time as compared to calculations made without this inner iteration.

Results and Discussion

The Cauchy integral and inverse boundary-layer analyses which are used to solve iteratively for the local interaction region near a transitional separation bubble were combined into a computer code referred to as ALESEP (Airfoil Leading-Edge Separation). The code is set up to input the displacement thickness and pressure distribution for the reference solution about which the local interaction analysis is assumed to be a linear perturbation. In this section, the results obtained with this analysis are compared with the experimental data of Gaster[4] and Gault[3] for transitional separation bubbles. The sensitivity to the transition model and the limits on the Cauchy integral are demonstrated in these results. In all of these calculations, 100 grid points were placed nonuniformly across the boundary layer with a minimum step size adjacent to the wall prescribed so as to provide an adequate resolution of the high gradient turbulent boundary layer which occurs downstream of the separation bubble. These calculations were initiated with an assumed linear distribution of the total displacement thickness and were continued until the difference between u_{e_l} and u_{e_v} was less than 0.2%. In general about 20 global viscous-inviscid interaction iterations were required. In most cases, the calculations were performed with a relaxation factor of unity.

Gaster Experiment

Gaster[4] performed a detailed experimental investigation on transitional separation bubbles which were induced on a flat plate by the pressure distribution which resulted from an airfoil placed near the plate. The particular case chosen from Gaster's report[4] is Series I, No. IV. The perturbation technique described in the analysis section was used in this calculation with the reference pressure, shown in Fig. 3a, set equal to that measured by Gaster with the boundary layer tripped from laminar to turbulent flow near the flat-plate leading edge. The reference displacement surface was computed from a direct calculation of the present finite difference boundary-layer procedure with the reference pressure distribution prescribed and instantaneous transition assumed at the experimental trip location.

In the viscous-inviscid interaction calculation, a streamwise mesh of 81 grid points was distributed in the interaction region, $0.5 \le s/L \le 1.5$, with a constant step size of $\Delta s/L = 0.0125$. In this particular case, the best agreement of the computed results with the experimental data was obtained with transition assumed to occur instantaneously at $s/L = 1.0$. Figure 3a shows excellent agreement between the computed pressure distribution upstream and downstream of the strong interaction region. It is observed in Fig. 3a that the presence of the transitional separation bubble slightly reduces the suction peak and results in a pressure plateau further downstream in the separated flow region. The "break" in the pressure curve occurs at the point where the flow was assumed to undergo instantaneous transition with a rapid recovery in

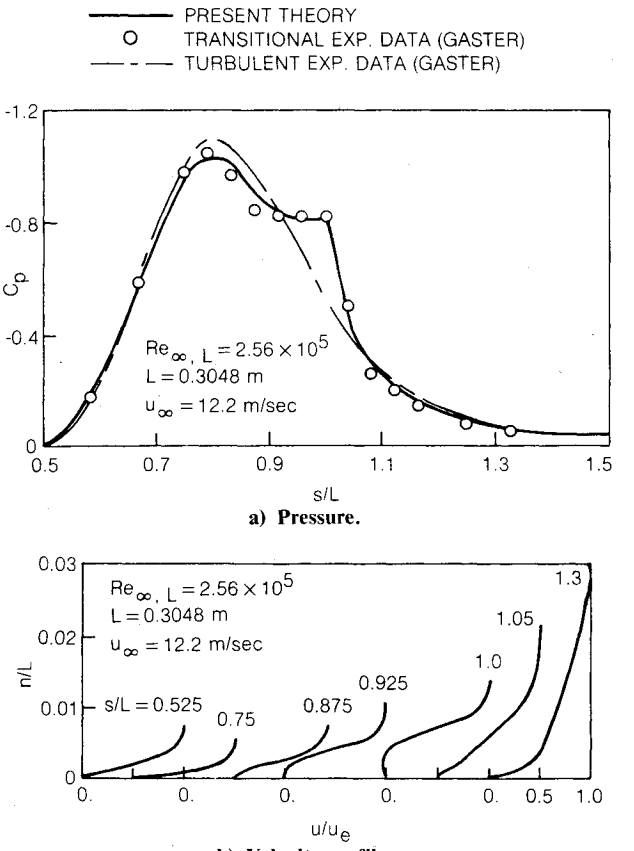

Fig. 3 Predicted results for Gaster case.

pressure taking place immediately downstream. Figure 4b, which will be discussed later in this section, shows excellent agreement in the predicted and measured separation and reattachment points. In addition, excellent agreement was observed between the predicted and measured momentum thickness Reynolds numbers at the separation point.

Figure 3b shows several of the velocity profiles computed in this case which illustrate the significant changes which occur in the shape of the profile over the interaction region. These profiles have been plotted only up to the n location where $u/u_e = 0.995$ in order to show the large streamwise growth which occurs in the boundary-layer thickness as the transition process takes place.

Numerical tests were performed to test the sensitivity of the interaction analysis to the specification of the transition region. Figure 4a shows the two intermittency distributions which were used in these calculations along with the instantaneous transition model that was used in the results discussed previously. For the case designated as "small transition region," the Dhawan and Narasimha intermittency function given in Eq. (22) was used with $s_{t_1} = 0.9395$ and $s_{t_2} = 1.158$; in the case referred to as "large transition region," the start and end of transition were specified by $s_{t_1} = 0.958$ and $s_{t_2} = 1.271$, respectively. Figure 4b shows the effects of the different transition regions on the computed skin friction; additional interaction results are presented in Ref. 16. These results show only small differences between the instantaneous and small transition region calculations; however, the computed interaction results differ significantly with the use of the intermittency distribution in the large transition region case. In this case, the onset of transition is delayed and the length scale of the transition region is increased as compared to the other two cases which results in a significant overprediction of the extent of the separated flow as shown in Fig. 4b. Although the large transition region model is not applicable to this particular case, the computed

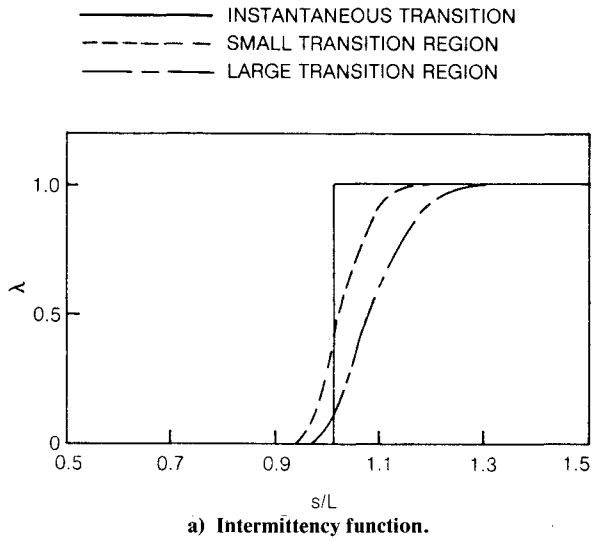

a) Intermittency function.

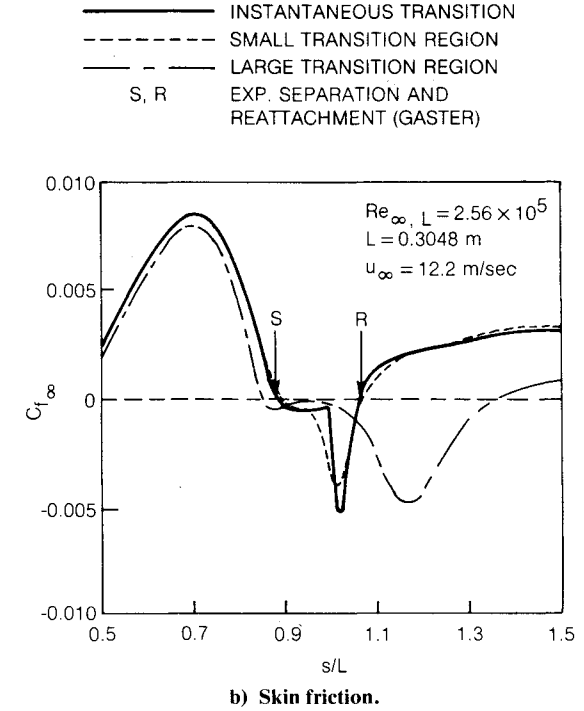

b) Skin friction.

Fig. 4 Effects of transition region on predicted results.

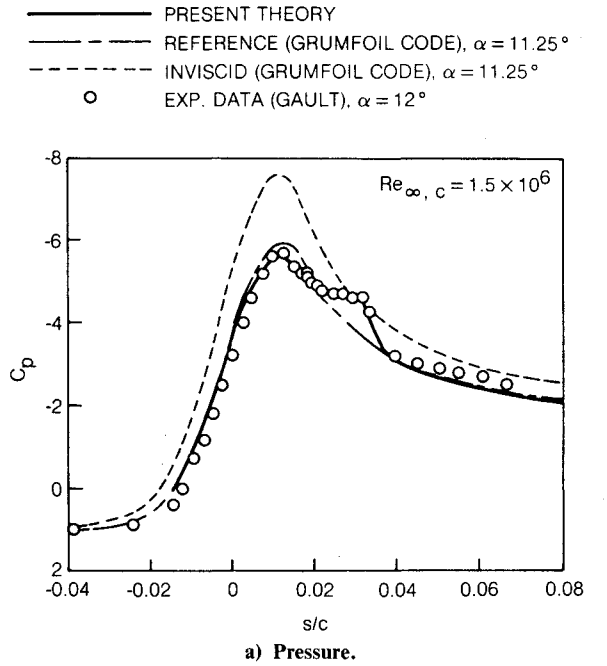

a) Pressure.

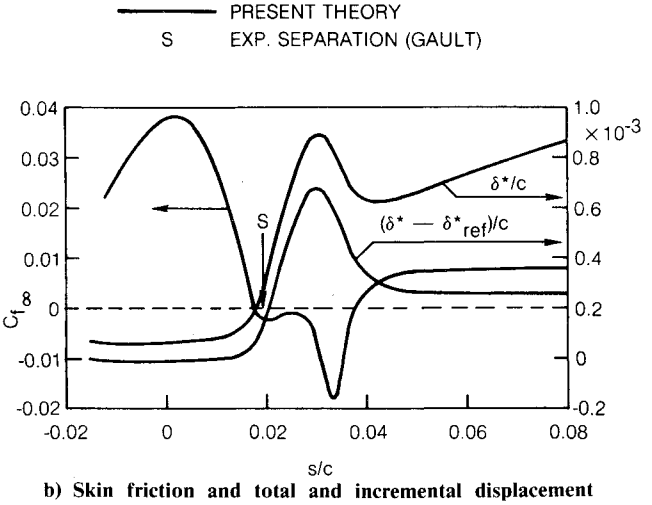

b) Skin friction and total and incremental displacement thickness.

Fig. 5 Predicted results for NACA 66_3-018 airfoil.

results show the correct qualitative behavior that would occur if transition were delayed due to a decrease in Reynolds number. Although not presented here, results were also obtained with the imposed transition region moved further upstream near the laminar separation point. As expected, these results show a significant underprediction in the extent of the separation bubble and subsequent interaction. It is concluded from this study that the use of the Dhawan and Narasimha intermittency function in the present interaction analysis produces physically correct results; however, further work clearly is required in order to obtain an analytical procedure which provides the onset and length of the transition region.

Gault NACA 66_3-018 Airfoil

Gault[3] made detailed experimental measurements of transitional bubbles on different airfoils at various flow conditions. Several comparisons are made with these data using the present localized interaction analysis. In the first case, an analysis was conducted for the transitional bubble which occurs at the leading edge of a NACA $66_3 - 018$ airfoil at a chord Reynolds number of 1.5×10^6 and 12-deg angle of attack. At this angle of attack, the reference solution, obtained from the GRUMFOIL code, was found to significantly overpredict the lift coefficient reported by Abbott and von Doenhoff[30] for this airfoil. Correspondingly, the pressures in the strong acceleration region were overpredicted, thereby providing an inaccurate reference solution for this case. These errors are probably due to the inability of the GRUMFOIL code to model correctly the lift decrement due to the massive trailing-edge separation which occurred in this case at 0.75 chord on the upper surface. In order to compensate for this problem, the GRUMFOIL code was run at a reduced angle of attack of 11.25 deg which provided a much better match of the experimental lift coefficient and the pressure distribution between the stagnation point and the peak suction region as shown in Fig. 5a.

The local interaction analysis was performed with a variable streamwise mesh of 78 grid points distributed over the interaction region $-0.0148 \le s/c \le 0.31$, where s is the arclength measured from the airfoil line of symmetry. In the present case, as well as the NACA 0010 (modified) airfoil case

to be discussed next, the arclength was measured along the actual airfoil surface instead of the reference displacement surface since these two surfaces are nearly coincident for these two cases. The transition region was imposed from $s_{t1}=0.0258$ to $s_{t2}=0.0432$ with the Dhawan and Narasimha intermittency function. The location of s_{t1} was placed approximately midway between the separation point and the "breakpoint" in the experimental pressure distribution; s_{t2} was located so that the intermittency function gave a value of $\lambda=0.5$ at the experimental pressure "breakpoint." With an assumed initial distribution of a linearly varying displacement thickness, it was found that the interaction calculation was unstable; however, this instability was eliminated and converged results were obtained in 50 global iteration cycles by using an underrelaxation factor of 0.5 on the perturbation mass flow parameter m in each cycle of the global iteration procedure shown in Fig. 2.

The computed results for this case are shown in Figs. 5a and 5b for the pressure, and skin friction and displacement thickness, respectively. Good agreement is obtained between the predicted results and Gault's pressure data and measured separation point for this case. Figure 5a also shows the inviscid airfoil pressure distribution which was obtained from the GRUMFOIL code with $\alpha=11.25$ deg. The large difference between this solution and the viscous airfoil solution obtained with the GRUMFOIL code shows the importance of including the viscous effects in the reference solution which is input to the present perturbation interaction analysis.

Two additional calculations were performed to test the sensitivity of the interaction analysis to the upstream and downstream limits on the Cauchy integral given in Eq. (2). In the first calculation, the lower limit was placed at $s_1/c=0$ with $s_2/c=0.31$ as was used earlier; in the second calculation, the upper limit was placed at $s_2/c=0.12$ with $s_1/c=-0.0148$ as was used earlier. These additional calculations resulted in no significant changes from those discussed previously, thereby verifying that in the present perturbation approach the numerical solution of the Cauchy integral can be confined to the interaction region. The point is further supported by Fig. 5b which shows the streamwise variation of the difference between the interacted and reference displacement thickness is nearly constant and thus provides virtually no contribution to the Cauchy integral source strength in these regions. It is observed in Fig. 5b that upstream of the interaction region, in the laminar portion of the flow, the displacement thickness increment differs slightly from zero, this small difference being due to the difference between the integral laminar boundary-layer analysis in the GRUMFOIL code and the present finite difference approach.

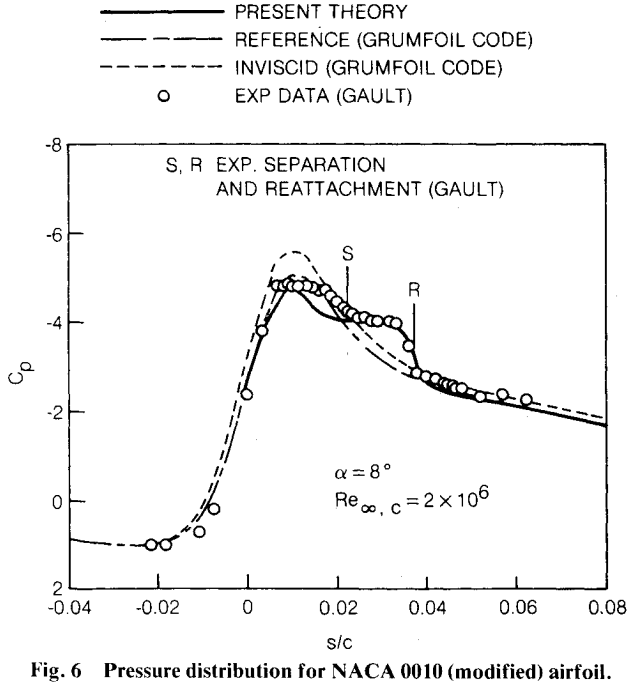

Fig. 6 Pressure distribution for NACA 0010 (modified) airfoil.

Gault NACA 0010 (Modified) Airfoil

Calculations were performed for this airfoil; tested experimentally by Gault[3] for an angle of attack of 8 deg and a chord Reynolds number of 2×10^6. The reference viscous airfoil solution obtained from the GRUMFOIL code gave good agreement with the experimental pressure distribution in the strong acceleration region ahead of the transitional separation bubble, as shown in Fig. 6. In this case, the turbulent separation at the trailing edge was less than 1% chord, thereby having no significant effect on the leading-edge pressure distribution. In the local interaction calculation 71 grid points were distributed nonuniformly in the interaction region, $0\le s/c\le0.32$, with the minimum grid spacing placed in the transition region. The transition region was imposed from $s_{t1}=0.0283$ to $s_{t2}=0.0444$ with the Dhawan and Narasimha intermittency function.

Comparison of the predicted pressure distribution and Gault's experimental data is shown in Fig. 6. Although the present analysis shows the same overall features as the data, the detailed agreement between the local interaction solution and Gault's data is not as good as that shown earlier for the NACA 66_3-018 airfoil. In this case, the data has a local constant pressure region in the peak suction region which was not obtained in either the interaction solution or the inviscid and reference solutions obtained from the GRUMFOIL analysis. A number of calculations were performed with different intermittency distributions to see if improved agreement could be obtained with the experimental data in the peak suction region. However, none of these assumed functions improved the agreement since this region is upstream of the experimental separation bubble indicated by S and R. Crimi and Reeves[12] also computed this case; however, their comparison with Gault's data was shown only in the immediate vicinity of the separated flow region so it is not clear as to whether or not they encountered the same disagreement in the peak suction region.

In Ref. 16, an additional comparison is presented with Gault's data at a chord Reynolds number of 4×10^6. Again the same constant pressure region was observed in the experimental data near the peak suction region which was not found in the interaction analysis. Despite these differences, it is shown[16] that the present analysis predicts the correct Reynolds number effect on the airfoil leading-edge separation bubble since the separation point moves only slightly for an increase in Reynolds number, whereas the upstream movement of the reattachment point is by about the same amount as that found experimentally by Gault.

Concluding Remarks

A local inviscid-viscous interaction technique has been developed for the analysis of low-speed, airfoil leading-edge transitional separation bubbles. In this analysis an inverse finite difference boundary-layer procedure is combined iteratively with a Cauchy integral representation of the inviscid flow which is assumed to be a linear perturbation to a known global viscous airfoil solution in the local interaction region. In this paper several comparisons have been made with experimental data for transitional separation bubbles. Overall, good agreement has been obtained in these comparisons which indicates the validity of the present local interaction technique. In contrast with existing global analyses, the present localized interaction analysis is demonstrated to be capable of resolving the details of the short leading-edge transitional bubbles which occupy only a few percent of the airfoil chord. In the future this interaction analysis should be applied over a wider range of flows to see if

the correct Reynolds number and angle-of-attack effects on airfoil transitional separation bubbles can be predicted.

In these comparisons a forced transition model has been used in which the onset and length of the transition region were specified a priori. Numerical tests were performed with this model which indicated that the flow is somewhat sensitive to the specified region. Whereas the use of a forced transition model allowed the assessment of the overall interaction model presented herein, in the future work should be directed at the development of a natural transition model for the prediction of transitional separation bubbles.

Acknowledgments

The authors express their gratitude to Mr. Joel L. Everhart, Technical Monitor, of the NASA Langley Research Center, for his assistance during the execution of this work, which was performed under NASA Contract NAS1-16585. In addition, the authors would like to thank Dr. R. E. Melnik of the Grumman Aerospace Corporation for making the GRUMFOIL code available for use in the present investigation.

References

[1] Tani, I., "Low Speed Flows Involving Bubble Separations," *Progress in Aeronautical Sciences*, Vol. 5, 1964, pp. 70-103.

[2] Bursnall, W. J. and Loftkin, L. K. Jr., "Experimental Investigation of Localized Regions of Laminar Boundary-Layer Separation," NACA TN 2338, April 1951.

[3] Gault, D. E., "An Experimental Investigation of Separated Laminar Flow," NACA TN 3505, Sept. 1955.

[4] Gaster, M., "The Structure and Behavior of Laminar Separation Bubbles," AGARD CP 4, 1966, pp. 819-854.

[5] Mueller, T. J. and Batill, S. M., "Experimental Studies of the Laminar Boundary Layer Separation Bubble on a Two-Dimensional Airfoil at Low Reynolds Numbers," AIAA Paper 80-1440, 1980.

[6] Owen, P. R. and Klanfer, L., "On the Laminar Boundary Layer Separation from the Leading Edge of a Thin Airfoil," Aeronautical Research Council, England, Current Paper 220, 1955.

[7] Horton, H. P., "A Semi-Empirical Theory for the Growth and Bursting of Laminar Separation Bubbles," Aeronautical Research Council, England Current Paper 1073, 1967.

[8] Roberts, W. B., "Calculation of Laminar Separation Bubbles and Their Effect on Airfoil Performance," *AIAA Journal*, Vol. 18, Jan. 1980, pp. 25-31.

[9] Stevens, W. A., Goradia, S. H., and Braden, J. A., "A Mathematical Model for Two-Dimensional Multi-Component Airfoils in Viscous Flows," NASA CR-1843, July 1971.

[10] Melnik, R. E., Chow, R., and Mead, H. R., "Theory of Viscous Transonic Flow Over Airfoils at High Reynolds Number," AIAA Paper 77-680, June 1977.

[11] Briley, W. R. and McDonald, H., "Numerical Prediction of Incompressible Separation Bubbles," *Journal of Fluid Mechanics*, Vol. 69, Pt. 4, 1975, pp. 631-656.

[12] Crimi, P. and Reeves, B. L., "Analysis of Leading-Edge Separation Bubbles on Airfoils," *AIAA Journal*, Vol. 14, Nov. 1976, pp. 1548-1555.

[13] Pletcher, R. H., Kwon, O. K., and Chilukuri, R., "Prediction of Separating Turbulent Boundary Layers Including Regions of Reversed Flow," Iowa State University, Ames, Iowa, ISU-ERI-Ames-80112, Final Tech. Rept. HTL-22, Feb. 1980.

[14] Gleyzes, G., Cousteix, J., and Bonnet, J. L., "Bulbe de Decollement Laminaire Avec Transition—Essai de Prévision Avec Couplage Local," AGARD Conference on Computation of Viscous-Inviscid Interactions, No. 21, AGARD CP-291, Oct. 1980.

[15] Cebeci, T., Stewartson, K., and Williams, P. G., "Separation and Reattachment Near the Leading Edge of a Thin Airfoil at Incidence," AGARD Conference on Computation of Viscous-Inviscid Interaction, No. 20, AGARD CP-291, Oct. 1980.

[16] Carter, J. E. and Vatsa, V. N., "Analysis of Airfoil Leading Edge Separation Bubbles," NASA CR-165935, May 1982.

[17] Napolitano, M., Werle, M.J., and Davis, R. T., "Numerical Solutions of the Triple-Deck Equations for Supersonic and Subsonic Flow Past a Hump," University of Cincinnati, Cincinnati, Ohio, Rept. AFL 78-6-42, June 1978.

[18] Carter, J. E., "Viscous-Inviscid Interaction Analysis of Transonic Turbulent Separated Flow," AIAA Paper 81-1241, 1981.

[19] Werle, M. J. and Verdon, J. M., "Viscid Inviscid Interaction of Symmetric Trailing Edges," Naval Air Systems Command, Washington, D.C., CR N00019-78-C-0604, Jan. 1980.

[20] Cebeci, T. and Smith, A. M. O., *Analysis of Turbulent Boundary Layers*, Academic Press, New York, 1974.

[21] Carter, J. E., "Inverse Boundary Layer Theory and Comparison with Experiment," NASA TP-1208, Sept. 1978.

[22] Reyhner, T. A, and Flügge-Lotz, I., "The Interaction of a Shock Wave with a Laminar Boundary Layer," *International Journal on Non-Linear Mechanics*, Vol. 3, No. 2, June 1968, pp. 173-199.

[23] van Ingen, J. L., "Transition, Pressure Gradient, Suction Separation and Stability Theory," Laminar-Turbulent Transition, Paper 20, AGARD CP-224, May 1977.

[24] Dhawan, S. and Narasimha, R., "Some Properties of Boundary Layer Flow During Transition from Laminar to Turbulent Motion," *Journal of Fluid Mechanics*, Vol. 3, 1958, pp. 418-436.

[25] Carter, J. E., "A New Boundary-Layer Inviscid Iteration Technique for Separated Flow," AIAA Paper 79-1450, July 1979.

[26] LeBalleur, J. C., "Couplage Visqueux-Non Visqueux: Method Numerique et Applications aux Ecoulements Bidimensionels Transsoniques et Supersoniques," *La Recherche Aerospatiale*, No. 1978-2, pp. 67-76.

[27] Kuhn, G. D., "An Improved Interaction Method for Exhaust Nozzle Boattail Flows," AIAA Paper 80-0197, Jan. 1980.

[28] Whitfield, D. L., Swafford, T. J., and Jacocks, J. J., "Calculation of Turbulent Boundary Layers with Separation and Viscous-Inviscid Interaction," *AIAA Journal*, Vol. 19, Oct. 1981, pp. 1315-1322.

[29] Davis, R. T. and Werle, M. J., "Progress on Interacting Boundary-Layer Computation at High Reynolds Number," *Conference on Numerical and Physical Aspects of Aerodynamic Flows*, edited by T. Cebeci, Springer-Verlag, New York, 1982, pp. 187-212.

[30] Abbott, I. H. and von Doenhoff, A. E., *Theory of Wing Sections*, Dover Publications, Inc., New York, 1959.